POAC'15
Trondheim, Norway

Proceedings of the 23rd International Conference on
**Port and Ocean Engineering under Arctic Conditions**
**June 14-18, 2015**
**Trondheim, Norway**

# STUDY OF LOCAL PRESSURE DISTRIBUTION AND SYNCHRONIZATION DURING FREQUENCY LOCK-IN

Gesa Ziemer [1,2], Clemens Deutsch [3]
[1] Hamburg Ship Model Basin (HSVA), D-22305 Hamburg, Germany
[2] Institute for Structural Dynamics, D-21307 Hamburg, Germany
[3] Bremen University of Applied Science, D-28199 Bremen, Germany

## ABSTRACT
A cylindrical compliant model was equipped with tactile sensors and exposed to drifting level ice in a series of model tests in the Large Ice Basin of HSVA. Different failure modes have been observed and the corresponding distribution of local pressures has been recorded. Under certain conditions, the structure was set into lock-in vibrations with a steady-state of load and response. Cross-correlation functions were used in order to monitor the synchronization between discrete areas located around the structure's circumference. In addition, frequency analysis of local loads reveals harmonic and sub harmonic frequencies in the local load spectra.
The paper describes the test setup used for the model tests in ice, quality and accurateness of the tactile sensor measurements, analysis procedure of the discrete areas and discussion of results.

## INTRODUCTION
Frequency Lock-In (FLI) is a topic which has been discussed in the ice engineering community over the past decades and is still under debate because the fundamental physical mechanisms leading to lock-in and keeping the lock-in condition alive are not fully understood yet. This lack of understanding aggravates the numerical representation of FLI and consequently prevents reliable prediction of its occurrence (Kärnä et al., 2013). Synchronization of failure around the circumference of an offshore structure is deemed decisive for the onset of lock-in vibrations. This assumption is supported by full scale measurements e.g. at Norströmsgrund Lighthouse (STRICE EU project) which show synchronization of loads on up to nine load measuring panels (e.g. studied by Palmer and Bjerkas, 2013). However, these panels are quite large and do not allow for detailed spatial analysis of loads.
A suitable technique to monitor local ice loads with higher spatial resolution is the application of tactile sensors. Such application has been described for experiments with full scale ice e.g. by Sodhi et al. (2006) and has also been tested in different laboratories for scaled model tests (e.g. Bechthold et al. (2014)). In the presented research, a previously used test setup for monitoring FLI at model scale (see Onken et al., 2013) has been equipped with tactile sensors and tested in the Large Ice Basin of HSVA. Aim of this study is to evaluate the practicability of using tactile sensors for the described problem and to define a testing and data processing procedure which can be used for future tests.

## PHYSICAL MODEL TESTS

The physical model which is used in the present research has been designed as part of the BRICE project and its capability of representing FLI at model scale has been proven in two test campaigns. Details concerning the physical test setup are described in Onken et al. (2013) and van het Hooft (2014). The setup is shown in Figure 1 and its main properties are summarized in Table 1. It basically consists of a rigid cylinder mounted to a support frame which is free to move on linear bearings in x- and y-direction with a certain stiffness defined by spring clusters.

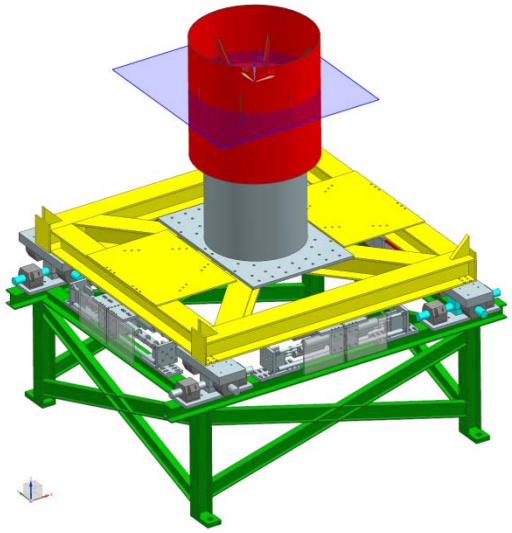

Table 1. Properties of the physical model.

| Property | Value |
|---|---|
| Diameter | 0.83 m |
| Translational stiffness in x- and y-direction at water level | 2282 N/mm |
| Natural Frequency (structure in the basin, no ice) | 5.12 Hz |

Figure 1: Sketch of the physical model.

### *Tactile Sensors*

In order to cover the full upstream half of the structure's circumference, three sensors of type 5260 from Tekscan are located next to each other at the ice-structure interaction area. Each sensor consists of 2288 pressure sensitive areas called "sensels", distributed in 44 rows and 52 columns. Each sensel has a size of 9.3 mm x 6.7 mm. Their maximum pressure range is 3.45 kPa per sensel, converted by 8 bit converter into 255 distinguishable load levels. The maximum pressure can be lowered according to the model test's needs, providing a better load resolution. The sensors are connected to Evolution Multiplexers for data acquisition and storage, allowing for sampling rates up to 100 Hz.

The sensors are made watertight by application of thin adhesive plastic foil and protected against ice abrasion by window safety foil. This procedure has been developed and tested by Bechthold et al. (2014).

### *Test Matrix*

Tests have been performed in level ice with a thickness of 45-50 mm, flexural strength 45-55 kPa and compressive strength 120-165 kPa. Velocities between 1 cm/s and 17 cm/s have been tested in order to monitor different failure mechanism. A total number of 15 test runs have been conducted.

## POST-PROCESSING OF TACTILE DATA

### *Equilibration*

An essential post-processing procedure for application of tactile sensors for the assessment of very small pressure fluctuations is the equilibration. Equilibration means that the whole sensor is loaded with a uniform pressure. Due to internal stress, varying wear of individual sensels and mechanical defects, sensels respond differently to this load due to slightly different sensitivity. Equilibration evens out such discrepancies and adjusts each cell such that the uniform load results in uniform sensel response. An example for equilibration is given in Figure 2. It shows an area of more sensitive sensels ("Hot Cells") in the middle of the sensor, which corresponds to the height of water level during the tests and is caused by more frequent cyclic loading of those sensels. Also, there is a diagonal line with less sensitive sensels which probably was caused by mechanical defects resulting from installation of the sensor on the structure.

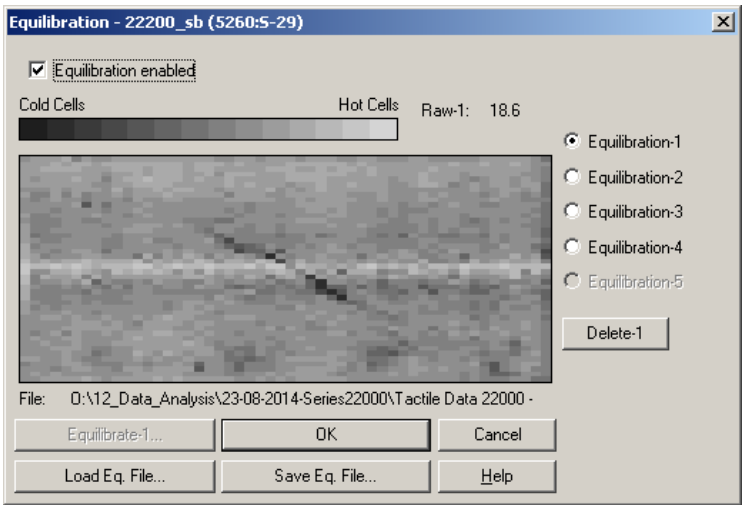


Figure 2. Visualization of equilibration (after testing).

### *Data Post-Processing*

Matrices obtained from the three individual tactile sensors are combined to one large matrix. Figure 3 shows an exemplary plot of combined local loads measured during an FLI event. Obviously, there are loaded sensels high above the water line which most probably result from internal stress of the sensors or intruded water. To remove these, a threshold is set which removes data from all sensels which are located more than twice the ice thickness higher than the waterline. All remaining sensel loads are integrated over the loaded height. Therefore, the ice load is treated as a line load. This is a major simplification, but the small thickness of the used model ice does not allow for spatial load analysis over ice thickness anyway. Data has been converted into a MATLAB data file for easier and faster handling.

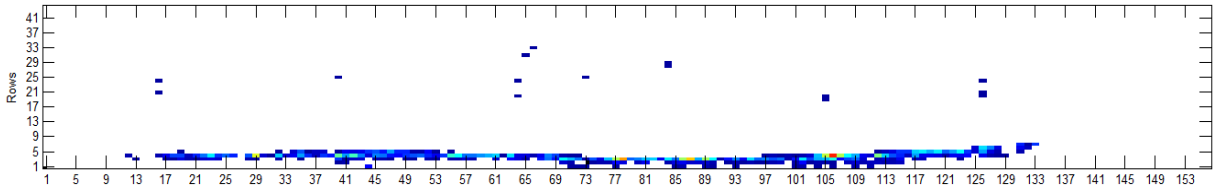


Figure 3. Example of loads measured by the tactile sensors.

### *Global Load Comparison*

To assess the correctness of the loads measured by the tactile sensors, the normal loads acting locally on all sensels are converted into a global ice force in ice drift direction, which is compared to ice forces measured by the six-component-scales. Note that the load cell measurements also include inertia forces which have to be removed from the measurements first. The used approach has been discussed by Onken et al. (2013). The comparison shows satisfying results regarding magnitude of total loads, but insufficient temporal resolution as illustrated exemplarily in Figure 4. High frequency fluctuations captured by the load cell sandwich (sampling rate 200 Hz) are not recognized by the tactile sensors.

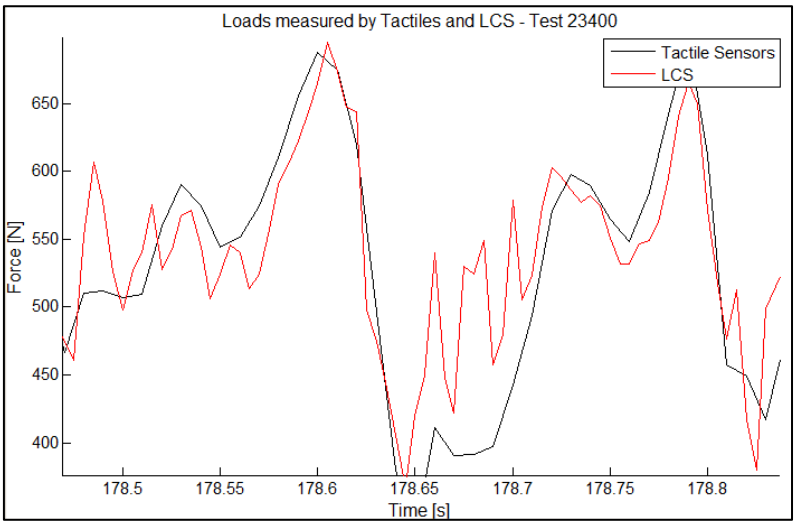


Figure 4. Comparison of load in ice drift direction measured by Tactile sensors (black) and 6-component load cell sandwich (red, without inertia forces).

## RESULTS

### *Considered Events*

The basic analysis presented in this paper deals with FLI events only. Therefore, suitable events were chosen according to following criteria:

1. Loading frequency equals frequency of response and is close to the natural frequency of the structure
2. Amplitudes of displacement are higher than 0.6 mm
3. The event has a duration of at least 4 seconds (corresponding to 20 cycles)

15 lock-in events have been found which match all requirements. They occurred at ice drift speeds between 2 and 5 cm/s and their load and response frequencies vary between 4.8 and 5.2 Hz. General observations explained in the following subsections refer to all of those events, although only a small number of them is illustrated in this paper.

### *Cross-Correlation*

The idea of lock-in being excited by synchronized failure around the circumference of the structure suggests a high cross-correlation of loads on individual discrete areas.

An example of cross-correlation factors during the steady state of FLI and their significance is given in Figure 5.

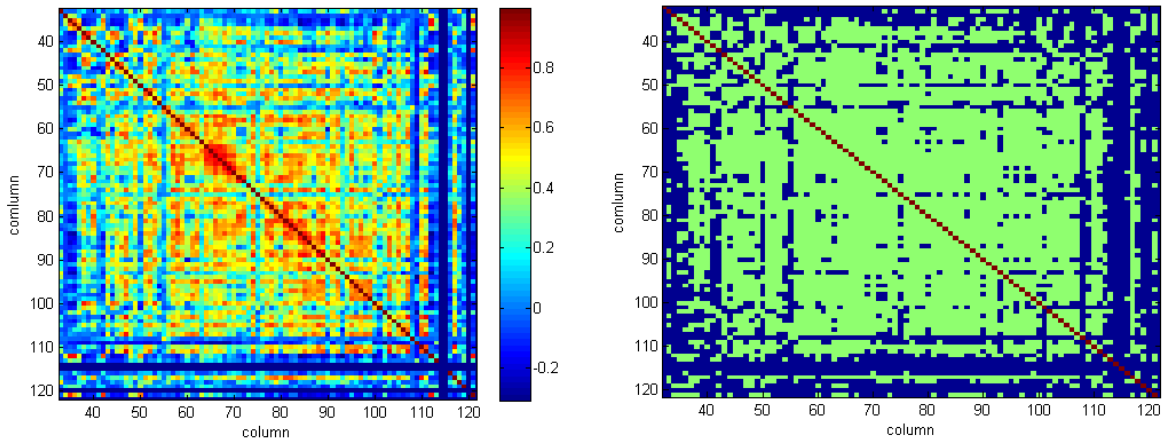


Figure 5. Left: Cross-correlation coefficients for individual sensels during a 8s FLI event. Only steady-state condition is taken into account. Right: Significance test for coefficients shown left. Green area indicates significance ($p<0.05$).

The overall correlation is high; however, the plot illustrates that neighbouring elements do not necessarily correlate and the correlation decreases towards the sides of the structure. But also in the centre part, some elements do not seem to be synchronized with the other areas.

The development of correlation during onset of FLI is illustrated by an example shown in Figure 6. The considered event is most suitable for such an analysis because it is the only occasion where failure de- and re-synchronizes. In all other events, FLI ends by global flexural failure of the ice. The corresponding correlation factors are presented and commented in Table 2.

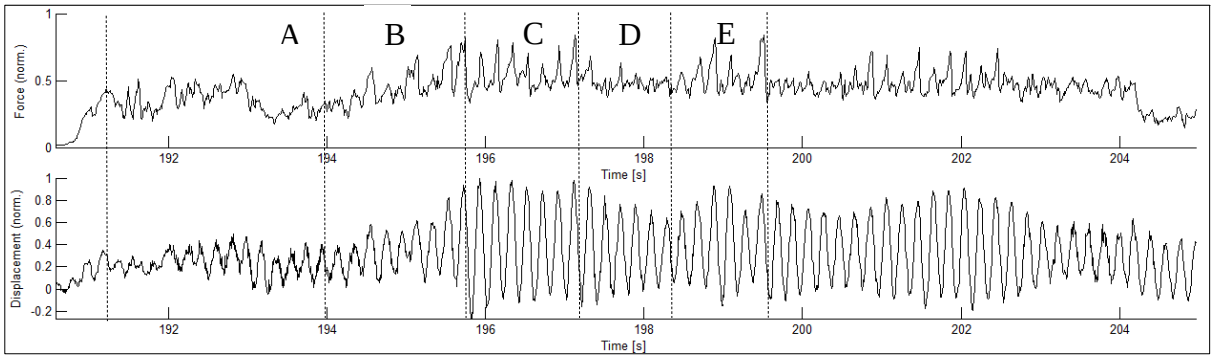


Figure 6. Top: Normalized total forces in ice drift direction, bottom: structural response.

Table 2. Crosscorrelation plots for time intervals indicated in Figure 4.

| Interval | Crosscorrelation Factors | Comment |
|---|---|---|
| A | 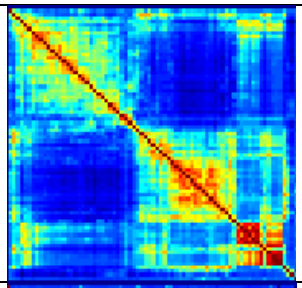 | Interval A begins when the ice starts interacting with the structure. No global synchronization has taken place. Correlation is high along the diagonal, meaning that ice on neighbouring sensels is likely to fail at the same time while sensels further apart experience a different load time history. |
| B | 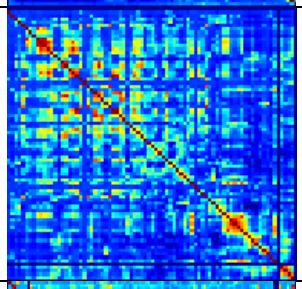 | The displacement measurement shows that the structure starts to shake severely during Interval B. The displacement amplitudes increase and all frequencies despite the structure's natural frequency diminish. The global correlation does not increase, but it is spread wider across the structure's circumference. Single areas are synchronizing. |
| C | 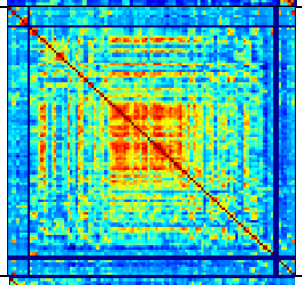 | Interval C contains 7 cycles of FLI. The overall correlation is much higher and is spread almost uniformly over the whole circumference, despite a clear area of maximum correlation at the center line, which corresponds to observations shown in Figure 5. |
| D | 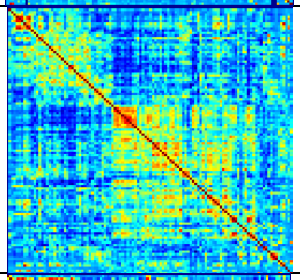 | For some reason, the high correlation at center line is not persistent and almost vanishes in Interval D. The global correlation stays at a high level compared to the condition before FLI. |
| E | 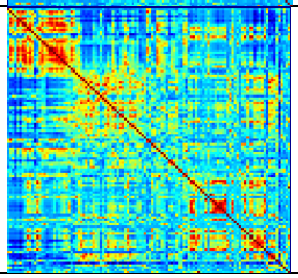 | A short and unsteady FLI event of 4 cycles takes place during Interval E. Again, the global correlation increases. The area of maximum correlation shifts from center to port side of the structure. |

The example shown above illustrates that load synchronization indeed is the key factor initiating lock-in and keeping lock-in alive. However, this does not necessarily mean that the ice fails simultaneously around the structure all at once. But it shows that parts of the loading and unloading mechanisms are synchronized.

***Spectral Analysis***

Cross-correlation plots reveal that the overall correlation increases during FLI, but sensels are not fully synchronized. This is further investigated by spectral analysis. An event is used which has a long duration and pronounced steady-state. The chosen event is shown in Figure 7. Despite a short interruption at t=99 s, the appearance of load and deflection is quite steady.

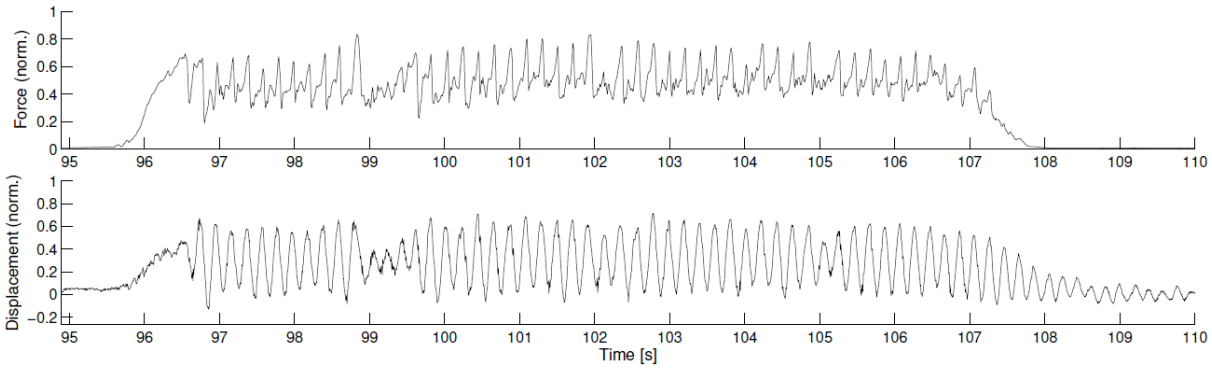


Figure 7. Top: Normalized total force in ice drift direction, bottom: structural response

Figure 8 shows FFT for global ice load and structural response. Next to the pronounced peak at 4.8 Hz, the load spectrum contains distinct peaks at 9.6 and 14.5 Hz, which are second and (close to) third harmonic of the natural frequency. Looking at FFT of individual sensels, also the first sub harmonic (2.4 Hz) is visible (Figure 9).

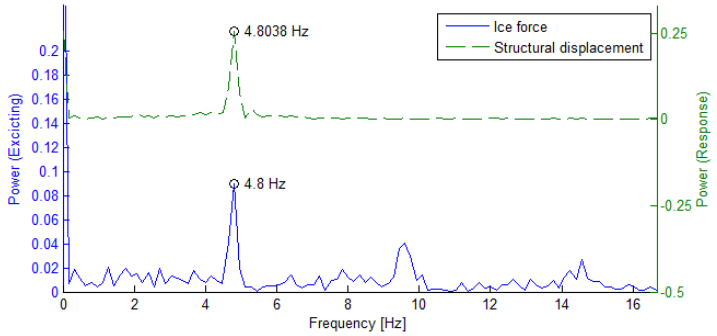


Figure 8. FFT for ice load and structural response during FLI event shown in Figure 5.

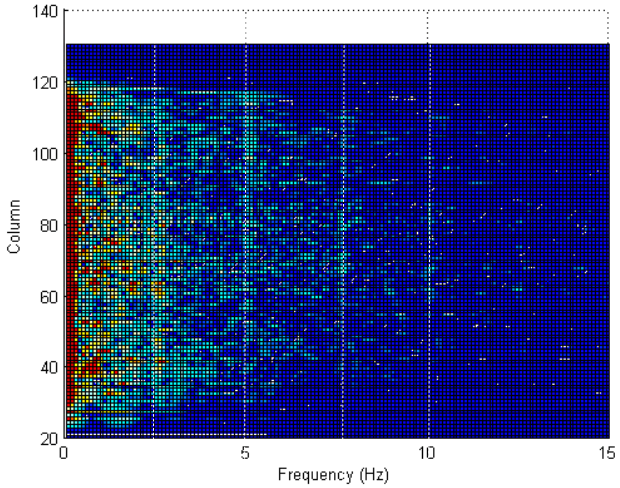


Figure 9. FFT for all individual sensels during FLI event shown in Figure 5. Magnitude of peak amplitude is indicated by colour.

***Time Domain Analysis***

The FFT and cross-correlation considerations suggest that the apparent simultaneous failure results from a superposition of individual failure loads which are not fully synchronized in time. This is illustrated by plotting loads on different scales, which is exemplarily done for a single loading and unloading cycle in Figure 10.

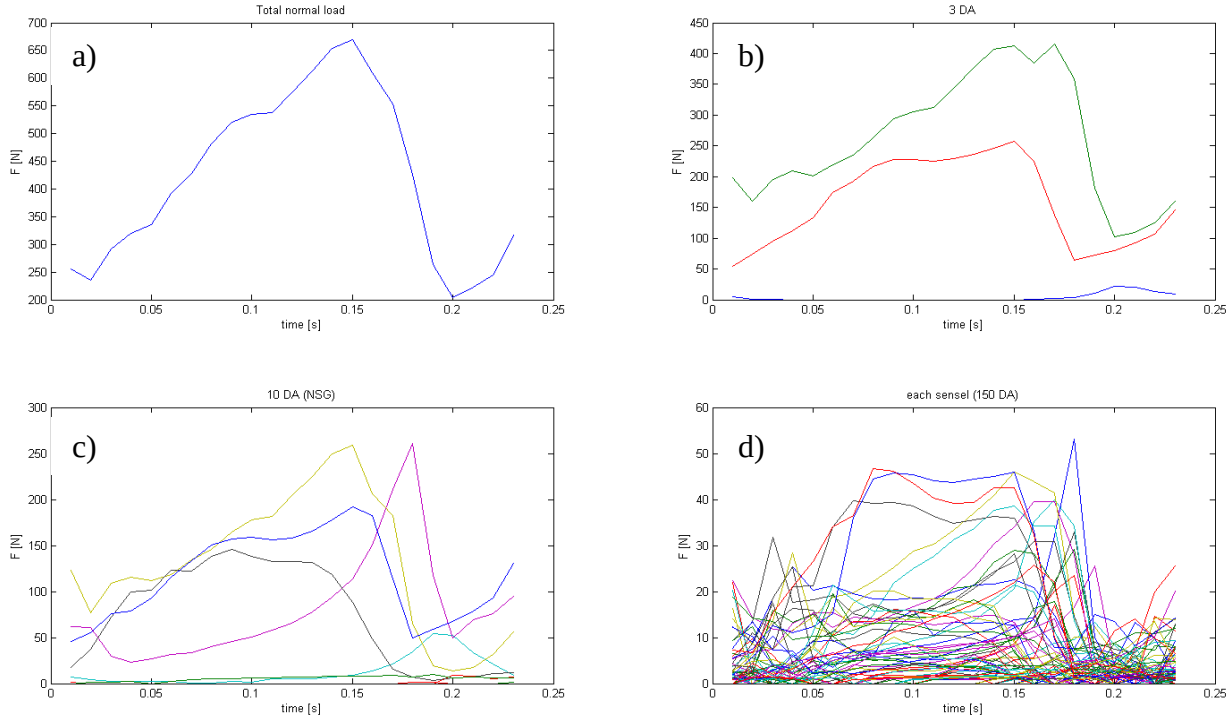


Figure 10. a) Total normal load (sum of all sensel loads) on 1.4m width of circumference, b) load split on the three sensors (each having a width of 0.48 m), c) load split into 10 discrete areas (width = 0.14 m), d) all sensel loads (width = 0.0093 m).

In Figure 10a, the total normal load is shown which has a saw-tooth shaped appearance with long build-up and rather short collapse phase. The build-up appears rather steady. Looking at each sensor individually (Figure 10b), one can see that the highest loads naturally appear on the front sensor (green), while the starboard sensor (blue) is not loaded, probably due to asymmetric ice contact after global failure. Ice on the front sensor fails later than ice on the port side sensor (red).

Figure 10c shows the sensors split up into 10 areas. One can see the saw-tooth shape on two of them (blue & yellow graph); having moderate load build-up and afterwards decreasing simultaneously. A third area (black) correlates to the build-up at first, but misses the high peak. It returns to a pressure value near zero earlier than the better synchronized areas, and the decrease takes longer. A fourth area (pink) also plays a significant role in the loading cycle which increases its load more rapidly and fails a little later than the other sections.

Figure 10d shows all individual sensel loads. Four different groups of sensels can be distinguished by the appearance of their loading and unloading time history:

1. Saw-tooth shape

   Some of the sensels show the saw-tooth shape one would expect from the FFT and the global load time history. Their cross correlation is high (e.g. light blue and yellow graphs).

2. Curved saw-tooth shape

   Sensels following the curved saw-tooth shape (similar to the pink graph in Figure 10c, e.g. dark blue in Figure 10d) have the same loading frequency as group 1, but with a small phase shift. They tend to fail a little later than the first group.

3. Plateau

   Some sensels show a rapidly increasing load at the beginning of the loading cycle and remain quite constant for half of the loading period. In the global load decrease phase they collapse first, significantly earlier than group 1 and 2. Examples for this group are the red and black graphs.

4. Random

   About 10% of the loaded sensels do not fit into any of the above mentioned groups. They tend to load and unload more frequent, but with no distinct periodicity.

## DISCUSSION

Tactile sensors prove to be a suitable solution for monitoring the interfacial processes during ice-structure interaction. Valuable data has been collected during the evaluation tests already and further investigation of the recorded local loads is required to extract more results and meaningful findings from it. The preliminary analysis presented in this paper reveals that at least for the structure that was subject to this specific test campaign, the local loads are less synchronized and shaped differently than anticipated beforehand. Apparently, there are different types of load shapes which lead to consecutive failure of the ice at different locations around the circumference of the structure. Further research is needed to evaluate whether such characteristic appears during FLI of structures with other dynamic properties as well, and to develop a theory about its formation.

Furthermore, the presented data lacks of high frequency processes which may alter the picture of individual sensel loads. For future test campaigns, the tactile sensors have to be used with hardware enabling higher sampling frequencies. Additionally, sensors with higher spatial resolution are required in order to monitor local loads over the height of the ice sheet as well, which is important to study the contact area.

## ACKNOWLEDGEMENTS

The authors would like to thank the HSVA ice tank crew for the professional execution of the tests. Furthermore, the authors wish to acknowledge Torodd S. Nord and Catherine Y. Pedersen from the Research Council of Norway supported Centre for Research-based Innovation SAMCoT, and the support of all SAMCoT partners. Their research has been an inspiration for the presented study, and their MATLAB routine has been a useful basis for the developed tactile measurement analysis MATLAB script.

## REFERENCES

Bechthold, J., Ziemer, G., Evers, K.-U., Jochmann, P., and Hoffmann, N. (2014). Study of local ice pressure distribution on a cylindrical offshore structure by using tactile sensors. In *Proceedings of the 22nd IAHR Int. Symp. on Ice*, Singapore.

Kärnä, T., Andersen, H., Gürtner, A., Metrikine, A., Sodhi, D., Loo, M., Kuiper, G., Gibson, R., Fenz, D., Muggeridge, K., Wallenburg, C., Wu, J.-F. and Jefferies, M., 2013. Ice-

induced vibrations of offshore structures – looking beyond ISO 19906. In *Proceedings of the 22nd Int. Conf. on Port and Ocean Engineering under Arctic Conditions,* Espoo, Finland.

Onken, G., Evers, K.-U., Haase, A. and Jochmann, P., 2013. Ice model tests with a cylindrical structure to investigate dynamic ice-structure interaction. In *Proceedings of the 22nd Int. Conf. on Port and Ocean Engineering under Arctic Conditions,* Espoo, Finland.

Palmer, A. and Bjerkas, M., 2013. Synchronization and the transmission from intermittent to locked-in ice-induced vibration. In *Proceedings of the 22nd Int. Conf. on Port and Ocean Engineering under Arctic Conditions,* Espoo, Finland.

Sodhi, D., Takeuchi, T., Nakazawa, N., Akagawa, S., and Saeki, H., 2006. Ice pressure measured during JOIA indentation tests. In *Proceedings of the 18$^{th}$ IAHR Int. Symp. on Ice,* Sapporo, Japan.

van het Hooft, M., 2014. *Experiments on Dynamic Ice-Structure Interaction.* M.Sc. Thesis, Delft University of Technology, Delft, The Netherlands.